RSC Advances

ROYAL SOCIETY OF CHEMISTRY

www.rsc.org/advances

Cite this: DOI: 10.1039/c0xx00000x

www.rsc.org/xxxxxx

ARTICLE TYPE

Synthesis of N-doped hierarchical carbon spheres for CO_2 capture and supercapacitors

ZiqiangWang,[abc] Lixian Sun,[ab*] Fen Xu,[b*] Xiaojun Peng,[c] Yongjin Zou,[b] Hailing Chu,[b] Liuzhang Ouyang,[d] Min Zhu[d]

Received (in XXX, XXX) XthXXXXXXXXX 20XX, Accepted Xth XXXXXXXXX 20XX

DOI: 10.1039/b000000x

N-doped hierarchical carbon spheres have been synthesized via soft template and hydrothermal method using melamine as a nitrogen source. The obtained carbon spheres possess high nitrogen content and well-developed porosity. These carbon spheres are examined as absorbents for CO_2 capture and as electrode materials for supercapacitors. Due to the high nitrogen content and hierarchical pore size distribution, the carbons show high CO_2 uptakes of 2.2-4.4 mmol g^{-1} at 298 K and 1 bar. Furthermore, we observe that the carbon spheres exhibit excellent performance as supercapacitor electrodes with a high specific capacitance of 356 F g^{-1} at a current density of 0.2 A g^{-1}. These carbon spheres as promising materials will exhibit excellent performance in various fields.

Introduction

The hierarchical carbon materials have attracted considerable attention owing to their high surface area, tunable porous structure, and excellent chemical and physical properties, which are widely applied in catalyst supports, gas storage and separation, and energy storage[1-4]. However, most of the carbon materials only possess a small fraction of specific active sites with highly hydrophobic surface, which impedes their practical applications. Thus many effects have been made to improve the surface property of the carbon materials. It has been reported that the incorporation of heteroatoms, such as boron, nitrogen, phosphorous and sulphur, into the carbon lattices has significant enhancement for the mechanical, field-emission, semiconducting, and electrical properties of carbon materials[5-9]. Recently, increasing heteroatom-doped carbon materials with a highly porous structure have been synthesized. Indeed, nitrogen as the most common element is usually incorporated into the carbon lattice to enhance the surface polarity, electric conductivity, and electron-donor tendency of the carbons, which is positive in CO_2 capture and separation, electric double-layer capacitors, and catalysis supports[10-13]. Additionally, the morphology of the carbons has a significant effect on their porous structure, properties and performance. The porous carbons with a spherical shape are favorable to minimize viscous effects and the energy required to pump and transport the suspension electrodes[14,15]. Moreover, carbon spheres with small diameters are expected to show better electrochemical performance due to their higher accessible surface area and better flow characteristics.

In general, N-doped hierarchical carbon spheres (NHCSs) are synthesized via the nanocasting approach employing mesoporous silica as a hard template, in which nitrogen-containing precursors are impregnated into the ordered mesoporous silica, followed by carbonization and removal of the silica template[16,17]. However, the hard-templating technology is time-consuming, high-cost, and unfeasible for mass production. Thus a reliable strategy to fabricate N-doped hierarchical carbon spheres is highly required. Recently, the hydrothermal carbonization (HTC) can be used to prepare the carbon spheres[18]. However, the hydrothermal method usually generates carbon materials with poor porosity and large particle size in the micrometer or millimeter scale. More recently, micro-mesoporous carbon spheres with the diameter of 3-6 μm were synthesized using polysaccharide carrageenan as a natural precursor via hydrothermal method[19]. Thus facile synthesis of N-doped hierarchical carbon spheres with high nitrogen content and small particle size still remains a great challenge.

Herein, we report a hydrothermal method to synthesize hierarchical carbon spheres using triblock copolymer F127 as a template and resol as a carbon source and melamine as a nitrogen source. The obtained NHCSs possess high surface area (561-1200 m^2 g^{-1}), hierarchical porous structure and high N content (up to 15.5 wt%). The nitrogen content is supplied by the introducing melamine into phenolic resin, where stable carbon nitrides are formed. The rigid frameworks can prevent the pore structure from collapse during the removal of the template and carbonization, leading to the formation of high surface area. Due to the high N content and hierarchical pore size distribution, the NHCSs show high CO_2 capture of 2.2-4.4 mmol g^{-1} at 298 K and 1 bar, and exhibit good performance as supercapacitor electrodes with specific capacitance of 356 F g^{-1} in 6 M KOH at a current density of 0.2 A g^{-1}.

Experimental Section

Preparation of N-doped hierarchical carbon spheres

N-doped hierarchical carbon spheres were prepared via a self-assemble route and performed at a mediate temperature

hydrothermal condition. The resol was synthesized according to the previous report[20]. In a typical synthesis, 10 g of phenol was melted at 40-42 °C, and 2.13 g of 20 wt% NaOH solution was added slowly under stirring for 10 min. After that, 17.7 g of formalin (ca. 37 wt%) was added, and the mixture was stirred at 70 °C for 60 min. Upon cooling down to room temperature, the pH value was adjusted to about 6 using 2 M HCl solution. Water was then removed under vacuum at 50 °C. The resol precursor was dissolved in ethanol (20 wt% ethanolic solution) to further separate sodium chloride as a precipitate. For the synthesis of the N-doped hierarchical carbon spheres, 2 or 4 g of melamine was dispersed in 50 mL of H_2O, and 2.6 g of formalin was added slowly under stirring, and reacted at 80 °C for 30 min. Then 2 g of F127 and 10 g of resol ethanol solution (20 wt%) were added and stirred for 2 h at 67 °C. Then 10 mL of the obtained solution was transferred into an autoclave and diluted with 20 mL of H_2O and reacted at 67 °C for 16 h and further heated at 130 °C for 24 h. The as-synthesized precursors were denoted MRF-1 and MRF-2, where 1 and 2 were the mass ratio of melamine to resol. The pyrolysis was carried out in a tubular furnace under Ar atmosphere at 600 °C for 2 h with a ramp rate of 2 °C min^{-1}. The samples were named NHCS-1 and NHCS-2 (N-doped hierarchical carbon spheres).

The chemical activation of N-doped hierarchical carbon spheres with KOH was performed to etch more pores. In a typical synthesis, 2 g NHCS-1 or NHCS-2 was immersed into 20 mL aqueous solution containing 4 g potassium hydroxide for 6 h. Then the solutions were dried in an oven at 100 °C under vacuum for 12 h. The obtained mixture was carbonized and activated under Ar up to a temperature of 600 °C (heating rate: 3 °C min^{-1}, holding time: 1 h). The activated samples were thoroughly washed with HCl (10 wt%) to remove inorganic salts and then washed with abundant distilled water until neutral pH. Finally, the carbons were dried in an oven at 105 °C. The activation samples were denoted A-NHCS-1 and A-NHCS-2.

Characterization

The morphology of N-doped hierarchical carbon spheres was examined by using scanning electron microscopy (JSM-6360LV, JEOL Ltd., Japan). Nitrogen sorption isotherms of carbon spheres were determined at 77 K using nitrogen in a conventional volumetric technique by a Quantachrome Autosorb-iQ_2 sorptometer. The surface area was calculated using BET method based on adsorption data in the relative pressure of 0.02-0.2, and total pore volume was determined from the amount of nitrogen adsorbed at the highest relative pressure (*ca*. 0.995). The micropore surface area and the micropore volume were obtained via t-plot analysis. The pore size distribution (PSD) was determined via a non-local density functional theory (NLDFT) method using a slit pore model with nitrogen adsorption data. Elemental analysis was obtained on a Vario III elemental analyzer. X-ray photoelectron spectroscopy (XPS) was gained from an ESCALAB 250Xi using standard Al Kα radiation (1486.6 eV) working at 278 W. The working pressure was 1×10^{-10} mbar.

CO_2 uptake

The CO_2 sorption isotherms of carbon spheres were measured by a Micromeritics ASAP2020 sorptometer. Highly purified carbon dioxide (99.999%) was used as the adsorbent for all the experiments. All samples were degassed at 200 °C for 12 h under vacuum. The CO_2 sorption isotherms were measured at 273 or 298 K.

Electrochemical Test

For the preparation of a working electrode, active materials (80 wt%), carbon black (10 wt%) and polytetrafluoroethylene (PTFE; 10 wt%) were mixed homogeneously, which was pressed onto nickel foam that served as a current collector. The mass of active materials was about 5 mg cm^{-2}. The electrochemical experiments were tested using a three-electrode cell, employing a platinum plate as the counter electrode, a saturated calomel electrode (SCE) (0.2415 V vs. the standard hydrogen electrode) as the reference electrode and 6 M KOH aqueous solution as the electrolyte. Cyclic voltammetry measurements were carried out on a Zahner IM6e electrochemical workstation at scan rates of 2-400 mV s^{-1} in a voltage range of -1 to 0 V. The galvanostatic charge/discharge tests were measured on a CHI 600E electrochemical workstation in the -1-0 V range at different current densities from 0.2 to 10 A g^{-1}.

Results and discuss

The morphologies of the precursors and carbon spheres were investigated by scanning electron microscopy. As shown in Fig. 1, the SEM images reveal that the precursors exhibit the spherical morphology with the size of 200 nm and cross-link each other due to the high surface energy. After carbonization and chemical activation at high temperature, the SEM images of carbons still exhibit spherical morphology with smooth surfaces, while the particle size gradually aggregate into large ones up to 0.5-1 μm. The carbons prepared with the melamine/resol = 1 show uniform dispersion while the carbons prepared with the melamine/resol = 2 possess agglomerated spherical particles, which may be caused by the cross-link of melamine residual. The results indicate that the high temperature and mild chemical activation have no effect on the morphology of carbons, but result in the enlargement of the particle size.

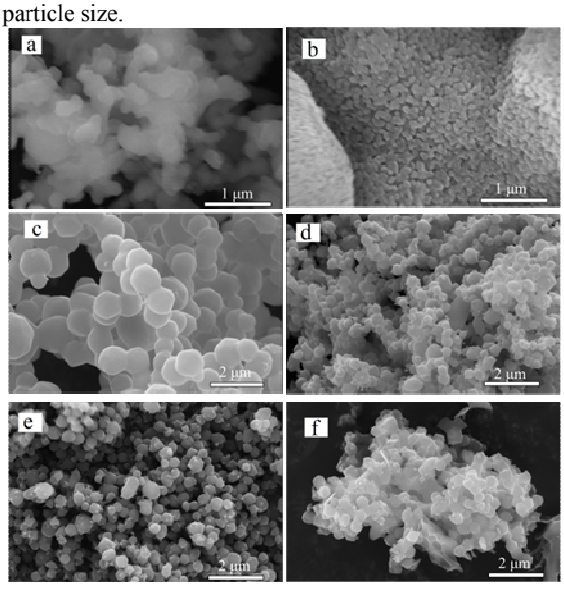

Fig. 1 SEM images of the precursors and carbon spheres (a: MRF-1; b: MRF-2; c: NHCS-1; d: NHCS-2; e: A-NHCS-1; f: A-NHCS-2).

The textural properties of the carbon spheres were analyzed by means of nitrogen sorption. The nitrogen sorption isotherms and corresponding PSD curves of carbon spheres are displayed in Fig. 2. All carbons exhibit steep uptakes at relative pressure (P/P_0) = 0.1 indicating the formation of abundant micropores. Furthermore, the N_2 sorption isotherms of the carbon spheres without chemical activation show a H_4-type hysteresis loop in the relative pressure range of 0.45–0.95 due to the capillary condensation in mesopores, which indicates the formation of uniform split mesopores. As the mass ratio of melamine to resol increases from 1 to 2, the nitrogen adsorption at low P/P_0 reduces and the hysteresis loop becomes large, indicating that the pore size gradually increases and the amount of mesopore increases. After chemical activation, the nitrogen adsorption at low P/P_0 increases and the hysteresis loop gradually becomes small, indicating the formation of more micropores and a shift of the mesopores to micropores. Due to the significant effect of the pore size on the CO_2 capture and supercapacitors, the pore size distribution of the carbon spheres was investigated. The PSD curves of the N-doped hierarchical carbon spheres, determined via a NLDFT method with a slit pore model using nitrogen adsorption data, exhibit that the micropores mainly locate in the ca. 0.6 and 1.2 nm and the mesopores concentrate in the ca. 2 and 4 nm. Furthermore, the chemical activation has a significant effect on the formation of pores. The mesopores at ca. 2 and 4 nm reduce while the micropores of 0.6 and 1.2 nm increase after chemical activation. This is because KOH activation of N-doped hierarchical carbon spheres can generate abundant micropores in the mesopore walls while some mesoporous channels collapse[21].

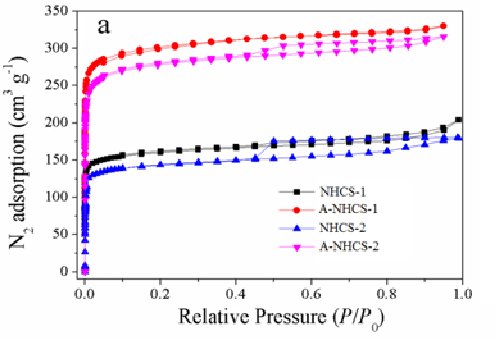

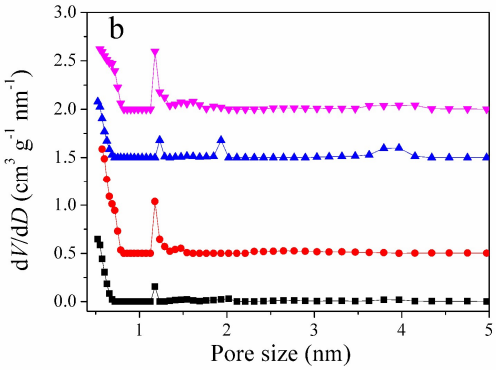

Fig. 2 Nitrogen sorption isotherms (a) and corresponding pore size distribution curves (b) of N-doped hierarchical carbon spheres.

The textural parameters of these carbon spheres are summarized in Table 1. As expected, a clear increase in the surface area and pore volume is observed after the chemical activation, indicating that the KOH activation play an active role in the generation of porosity for carbons. The surface area increases from 627 for NHCS-1 to 1200 m^2 g^{-1} for A-NHCS-1, and from 561 for NHCS-2 to 1101 m^2 g^{-1} for A-NHCS-2. The pore volume increases from 0.32 for NHCS-1 to 0.51 cm^3 g^{-1} for A-NHCS-1, and from 0.28 for NHCS-2 to 0.49 cm^3 g^{-1} for A-NHCS-2. Furthermore, it can be seen from the Table 1 that the pore size of carbon spheres are consist of abundant micropores and a small fraction of mesopores that are beneficial for CO_2 and supercapacitors by providing a highly accessible pathway to CO_2 molecules or electrolyte ions.

Table 1 Textual properties of precursors and the N-doped hierarchical carbon spheres.

Samples	Textural properties			N content	CO_2 uptake
	S_{BET} (m_2 g_{-1})[a]	V_t (cm^3 g^{-1})[b]	Maxima (nm)[c]	(wt%)	(mmol g^{-1})[d]
MRF-1	—	—	—	28.2	—
MRF-2	—	—	—	33.5	—
NHCS-1	627(545)	0.32(0.21)	0.6/1.2/2.1	8.2	2.2(3.4)
NHCS-2	561(479)	0.28(0.19)	0.7/1.2/1.9/3.9	15.5	2.5(3.5)
A-NHCS-1	1200(1076)	0.51(0.41)	0.6/1.2	7.7	3.4(4.9)
A-NHCS-2	1101(991)	0.49(0.38)	0.7/1.2/3.9	9.3	4.4(6.1)

[a]Values in parentheses are micropore surface area. [b]Values in parentheses are micropore volume. [c]Maxima of the pore size distribution are calculated by the NLDTF model. [d]The values in parentheses are obtained at 0 °C and 1bar.

In order to investigate the chemical property of N-doped hierarchical carbon spheres, elemental analysis and XPS were carried out to measure their chemical composition and structure. As listed in Table 1, the precursors have the high nitrogen content up to 28.2 and 33.5 wt% for MRF-1 and MRF-2, and the nitrogen content rapidly decreases to 8.2 and 15.5 wt% for NHCS-1 and NHCS-2 after carbonization, respectively. The result suggests that the heat treatment should lead to the decrease of nitrogen content due to the poor thermal stability of nitrogen groups. The nitrogen content of activated samples continually reduces to 7.7 and 9.3 wt% for A-NHCS-1 and A-NHCS-2, respectively, which is ascribed to the easy oxidation of nitrogen groups with KOH. The nature of the nitrogen species on the surface of the carbons was investigated by X-ray photoelectron spectroscopy (XPS). The XPS survey spectrum of the A-NHCS-2 exhibits strong signals of carbon, nitrogen and oxygen elements (Fig. 3a). The nitrogen content is about 8.8 wt%, corresponding with the results of the elemental analysis. This indicates that the nitrogen element is homogeneously distributed in the frameworks of the N-doped hierarchical carbon spheres. The N1s core level spectra of the A-NHCS-2 are shown in Fig. 3b. The A-NHCS-2 exhibits two peaks at the binding energy of 397.5 and 399.2 eV, which can be assigned to nitride-like species or aromatic N-imines[22,23], and $PhNH_2$ or –C=NH[24,25]. The two types of nitrogen are basic groups, and the contents of the two types of nitrogen group are 58% and 42%, respectively. The nitrogen covalently bonded with carbon can change the electroneutrality of carbon via conjugation with lone-pair electrons of nitrogen, leading to the increase of electric conductivity and the electron donor/acceptor property[26]. Therefore, the N-doped hierarchical carbon spheres with high basic nitrogen content can improve the performance for CO_2 capture and supercapacitor electrodes, as these basic nitrogen functionalities can act as an anchor for CO_2 capture or contribute pseudocapacitance through redox reaction.

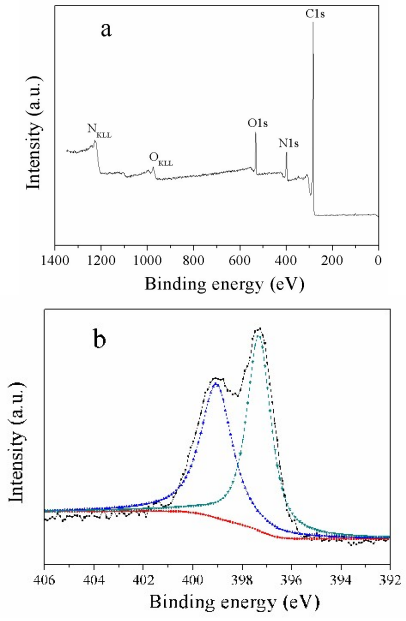

Fig. 3 XPS spectra of the A-NHCS-2: a) survey spectrum; b) N 1s spectra.

Recently, carbon dioxide capture and storage have attracted considerable attention due to the climate change caused by CO_2 emission. Fig. 5 shows the CO_2 adsorption isotherms of carbon spheres in the range of 0-1 bar. The CO_2 uptakes measured at 273 and 298 K are in the 3.3-6.1 and 2.2-4.4 mmol g^{-1} ranges, respectively. This is mainly due to their high nitrogen content and hierarchical pore size distribution. Indeed, the A-NHCS-2 with high surface area (1101 m^2 g^{-1}) and nitrogen content (9.3 wt%) exhibits a large capacity of 4.4 mmol g^{-1} at 298 K, which is superior to most porous carbons lately reported in the literatures[27-31]. The carbon spheres without chemical activation have low CO_2 uptakes (2.2 mmol g^{-1} for NHCS-1 and 2.5 mmol g^{-1} NHCS-2) at 298 K and 1 bar. Importantly, the carbon spheres with chemical activation have a sharp increase in CO_2 adsorption capacity (3.4 mmol g^{-1} for A-NHCS-1 and 4.4 mmol g^{-1} for A-NHCS-2). The results demonstrate that the porosity of the carbons has a significant effect on the CO_2 adsorption. Furthermore, the N-doped hierarchical carbon spheres with similar porosity possess higher nitrogen content resulting in larger CO_2 uptake capacity, which indicate that the basic nitrogen species have a significant contribution for CO_2 adsorption. This is because the nitrogen atom in the carbon lattices can change the electronic structure of carbon layer which has a strong reaction with CO_2 molecules due to the pole-pole interactions between the large quadrupole moment of CO_2 molecules (13.4×10^{-40} C m^2) and the polar sites related to nitrogen groups[32,33]. To illustrate the strength of the interaction between CO_2 and carbon materials, the isosteric heat of adsorption (Q_{st}) was calculated from the Clausius-Clapeyron equation using CO_2 adsorption isotherms at 273 and 298 K (See ESI*). At the onset of adsorption, the Q_{st} of A-NHCS-2 is 42.4 kJ mol^{-1} (Fig. S1). However, the Q_{st} gradually decreases to 25.6 kJ mol^{-1} when the CO_2 uptakes increase to 2.5 mmol g^{-1}, and then remains constant throughout the adsorption process. These results indicate that the excellent CO_2 adsorption performance for N-doped carbons is due to the large amount of nitrogen groups and well-developed porosity.

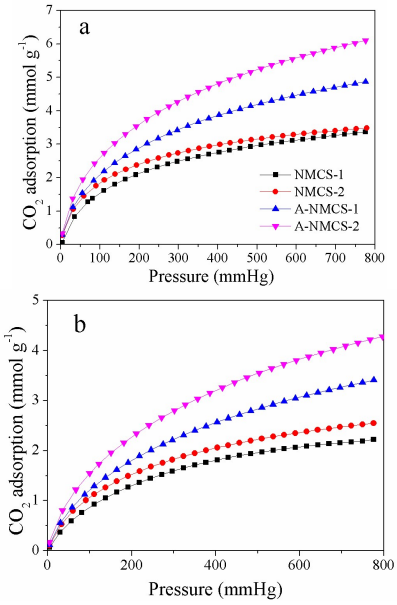

Fig. 4 Carbon dioxide adsorption isotherms of N-doped hierarchical carbon spheres at 273 (a) and 298 K (b).

For industrial applications, besides the high CO_2 adsorption, the selectivity of CO_2 over N_2 must be considered. As shown in Fig. S2, CO_2 and N_2 uptakes for A-NHCS-2 are 4.4 and 0.5 mmol g^{-1} at 298 K, respectively. The selectivity of CO_2 over N_2 is calculated from the ratio of the initial slopes of CO_2 and N_2 adsorption isotherms, which is as high as 23:1, indicating the successful separation of CO_2 from N_2 by the A-NHCS-2.

The as-synthesized N-doped hierarchical carbon spheres were also evaluated for electrode materials in supercapacitors. The cyclic voltammetry and galvanostatic charge/discharge tests were employed to characterize the capacitive properties. Fig. 6a shows the cyclic voltammetry curves of the A-NHCS-2 at a scan rate from 2 to 400 mV s^{-1}. The cyclic voltammetry shows a nearly rectangular shape in the low scan rate, suggesting a double-layer capacitance behavior. However, the shape has a great change that a polarization rectangular shape is formed at high scan rate due to the confined movement of the electrolyte ions in the micropores at high scan rate. Moreover, CV curves have wide humps in the range of -0.7 — -0.3 V, which can be attributed to the redox reaction induced by the incorporation of nitrogen atom into carbons. The charge-discharge plots of the A-NHCS-2 measured at a current density from 0.2 to 10 A g^{-1} are shown in Fig. 6b. The charge-discharge curves of the N-doped hierarchical carbon spheres have a slight arc shape with an IR drop due to the low conductivity of the electrode materials. The specific capacitance of the A-NHCS-2 is calculated from the discharge curves. The specific capacitance measured at a current density of 0.2 A g^{-1} is 356 F g^{-1} due to the combined contribution from double-layer capacitance and redox pseudocapacitance, which is better than that of most highly porous carbons recently reported in the literatures[34-37]. The specific capacitance of the A-NHCS-2 retains 55 % when the current density increases to 10 A g^{-1} (Fig. S3). The capacitance drop at high current density can be illustrated from the assumption that the charge diffusion in the pores is interrupted by the time constraint owing to the fast charging/discharging. For the estimating the cycle life of the A-NHCS-2, 5000 charge/recharge cycles at a current density of 10 A g^{-1} were carried out. As shown in Fig. 4S, the capacitance of the A-NHCS-2 retains 91% of its initial capacitance after 5000 cycles, indicating a well cycle stability of the electrode.

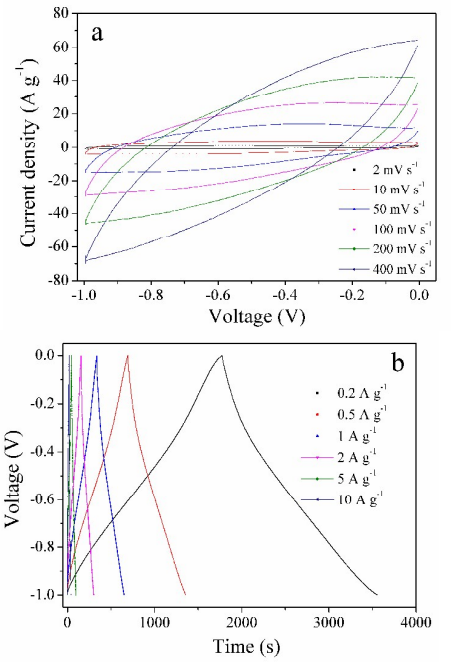

Fig. 5 Electrochemical performance of the A-NHCS-2 using a three-electrode cell in 6 M KOH: cyclic voltammograms at different scan rates (a) and galvanostatic charge/discharge curves at different current densities (b).

Conclusions

In summary, we demonstrate a facile two-step synthetic route for the synthesis of N-doped hierarchical carbon spheres using melamine as a nitrogen source and F127 as the soft template. The obtained carbon spheres possess high surface area (561-1200 m^2 g^{-1}), large amount of ultra-micropores (< 1 nm), and high nitrogen content (up to 15.5 wt%). Ascribed to their high nitrogen content and large surface area, the carbon spheres exhibit excellent performance as absorbents for CO_2 adsorption (2.2-4.4 mmol g^{-1} at 298 K and 1 bar) and as supercapacitor electrodes with high specific capacitance (356 F g^{-1}) in 6 M KOH at a current density of 0.2 A g^{-1}. These N-doped hierarchical carbon spheres as promising materials will be suitable for practical applications in a range of fields.

Acknowledgements

The authors wish to acknowledge the financial support from the NSFC (51361005, 21173111, 51371060, 51201042 and 51201041), Guangxi Natural Science Foundation (2014jjDA20005, 2014jjAA60035), Guangxi Key Laboratory of Information Materials (1210908-217-Z) and Guangxi Scientific Technology Team (2012GXNSFGA06002).

Notes and references

[a] *Dalian Institute of Chemical Physics, University of Chinese Academy of Sciences, 457 Zhongshan Road, Dalian 116023, P.R. China. E-mail: sunlx@guet.edu.cn, Tel: +867732303763, Fax: +867732290129*

[b] *Guangxi Key Laboratory of Information Materials, Guangxi Collaborative Innovation Center of Structure and Property for New Energy and Materials, School of Material Science and Engineering, Guilin University of Electronic Technology, Guilin 541004, P.R. China*

[c] *State Key Laboratory of Fine Chemicals, Dalian University of Technology, Dalian 116024, China*

[d] *School of Materials Science and Engineering, South China University of Technology, Guangzhou 510006, China*

† Electronic Supplementary Information (ESI) available: the detailed information of the calculation of isosteric heat of CO_2 adsorption and Fig. S1-S4 include here.

1. Z. Ling, G. Wang, M. D. Zhang, X. M. Fan, C. Yu, J. Yang, N. Xiao and J. S. Qiu, *Nanoscale,* 2015, **7**, 5120-5125.
2. Y. Xiao, H. Dong, B. Lei, H. Qiu, Y. Liu and M. Zheng, *Mater. Lett.*, 2015, **138**, 37-40.
3. W. Wang and D. Yuan, *Sci. rep.*, 2014, **4**, 5711.
4. J. Wang, H. L. Xin and D. Wang, *Part. Part. Syst. Char.*, 2014, **31**, 515-539.
5. V. V. Strelko, V. S. Kuts and P. A. Thrower, *Carbon*, 2000, **38**, 1499-1503.
6. D.W. Wang, F. Li, Z.-G. Chen, G. Q. Lu and H.M. Cheng, *Chem. Mater.*, 2008, **20**, 7195-7200.
7. S. Maldonado and K. J. Stevenson, *J. Phys. Chem. B*, 2005, **109**, 4707-4716.
8. U. B. Nasini, V. G. Bairi, S. K. Ramasahayam, S. E. Bourdo, T. Viswanathan and A. U. Shaikh, *J. Power Sources*, 2014, **250**, 257-265.
9. J. P. Paraknowitsch and A. Thomas, *Energy Environ. Sci.*, 2013, **6**, 2839-2855.
10. D. Hulicova-Jurcakova, M. Seredych, G. Q. Lu and T. J. Bandosz, *Adv. Funct. Mater.*, 2009, **19**, 438-447.
11. J. D. Wiggins-Camacho and K. J. Stevenson, *J. Phys. Chem. C*, 2009, **113**, 19082-19090.
12. J. Wei, D. Zhou, Z. Sun, Y. Deng, Y. Xia and D. Zhao, *Adv. Funct. Mater.*, 2013, **23**, 2322-2328.
13. H. Niwa, K. Horiba, Y. Harada, M. Oshima, T. Ikeda, K. Terakura, J. I. Ozaki and S. Miyata, *J. Power Sources*, 2009, **187**, 93-97.
14. X. Ma, M. Liu, L. Gan, Y. Zhao and L. Chen, *J. Solid State Electro.*, 2013, **17**, 2293-2301.
15. N. P. Wickramaratne, J. Xu, M. Wang, L. Zhu, L. Dai and M. Jaroniec, *Chem. Mater.*, 2014, **26**, 2820-2828.
16. Y. D. Xia and R. Mokaya, *Adv. Mater.*, 2004, **16**, 886-891.
17. S. Ikeda, K. Tachi, Y. H. Ng, Y. Ikoma, T. Sakata, H. Mori, T. Harada and M. Matsumura, *Chem. Mater.*, 2007, **19**, 4335-4340.
18. Y. Mi, W. Hu, Y. Dan and Y. Liu, *Mater. Lett.*, 2008, **62**, 1194-1196.
19. Y. Fan, X. Yang, B. Zhu, P. F. Liu and H. T. Lu, *J. Power Sources*, 2014, **268**, 584-590.
20. Y. Fang, D. Gu, Y. Zou, Z. Wu, F. Li, R. Che, Y. Deng, B. Tu and D. Zhao, *Angew. Chem. Int. Edit*, 2010, **49**, 7987-7991.
21. J. Wang and S. Kaskel, *J. Mater. Chem.,* 2012, **22**, 23710-23725.
22. D. N. Hendrickson, J. M. Hollander and W. L. Jolly, *Inorg. Chem.*, 1969, **8**, 2642-2647.
23. J. R. Pels, F. Kapteijn, J. A. Moulijn, Q. Zhu and K. M. Thomas, *Carbon*, 1995, **33**, 1641-1653.
24. S. Biniak, G. Szymanski, J. Siedlewski and A. Swiatkowski, *Carbon*, 1997, **35**, 1799-1810.
25. F. Kapteijn, J. A. Moulijn, S. Matzner and H. P. Boehm, *Carbon*, 1999, 37, 1143-1150.
26. H. Chen, F. Sun, J. Wang, W. Li, W. Qiao, L. Ling and D. Long, The *J. Phys. Chem. C*, 2013, 117, 8318-8328.
27. H. Cong, M. Zhang, Y. Chen, K. Chen, Y. Hao, Y. Zhao and L. Feng, *Carbon*, 2015, 92, 297-304.
28. L. Wan, J. Wang, C. Feng, Y. Sun and K. Li, *Nanoscale*, 2015, 7, 6534-6544.
29. B. Huang, H. Shao, N. Liu, Z. J. Xu and Y. Huang, *RSC Adv.*, 2015, 5, 88171-88175.
30. S. Zhang, Z. Li, K. Ueno, R. Tatara, K. Dokko and M. Watanabe, *J. Mater. Chem. A.*, 2015, 3, 17849-17857.
31. A. Alabadi, S. Razzaque, Y. Yang, S. Chen and B. Tan, *Chem. Eng. J.*, 2015, 281, 606-612.
32. W. Xing, C. Liu, Z. Zhou, L. Zhang, J. Zhou, S. Zhuo, Z. Yan, H. Gao, G. Wang and S. Z. Qiao, *Energy Environ. Sci.*, 2012, **5**, 7323-7327.
33. D. M. D'Alessandro, B. Smit and J. R. Long, *Angew. Chem. Int. Edit*, 2010, **49**, 6058-6082.
34. L. Wang, Z. Gao, J. Chang, X. Liu, D. Wu, F. Xu, Y. Guo and K. Jiang, *ACS Appl. Mater. Interfaces*, 2015, 7, 20234-20244.
35. H. Chen, D. Liu, Z. Shen, B. Bao, S. Zhao and L. Wu, *Electrochim. Acta*, 2015, 180, 241-251.
36. G. Ma, Q. Yang, K. Sun, H. Peng, F. Ran, X. Zhao and Z. Lei, *Bioresour. Technol.*, 2015, 197, 137-142.
37. Y. T. Li, Y. T. Pi, L. M. Lu, S. H. Xu and T. Z. Ren, *J. Power Sources*, 2015, 299, 519-528.

Table of entry

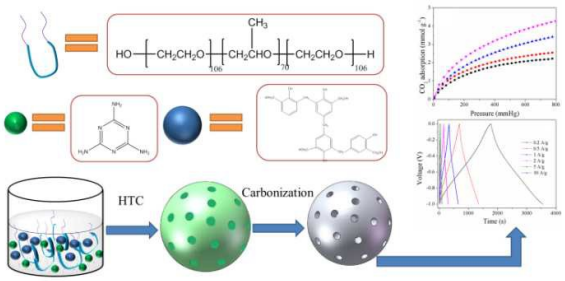

N-doped hierarchical carbon spheres prepared from soft template/hydrothermal method exhibit excellent performance for CO_2 capture and supercapacitors.